Available online at www.sciencedirect.com

SciVerse ScienceDirect

Physics Procedia 39 (2012) 674 – 682

Physics Procedia

LANE 2012

Periodic nanostructure formation on silicon irradiated with multiple low-fluence femtosecond laser pulses in water

Kenzo Miyazaki*, Godai Miyaji

Institute of Advanced Energy, Kyoto University, Gokasho, Uji, Kyoto 611-0011, Japan

Abstract

It is shown that superimposed multiple shots of linearly polarized 800-nm, 100-fs laser pulses at lower fluence than the single-pulse ablation threshold produce periodic nanostructures with almost constant periods of 150 nm and 400 nm on silicon surface immersed in water. The nanostructure formation and its characteristic properties observed are illustrated well with the excitation of surface plasmon polaritons in the newly created surface layer. Pump and probe measurements of surface reflectivity during the ultrafast interaction demonstrate that multiple shots of low-fluence fs pulses are crucial to the accumulation of non-thermal bonding structure change and subsequent ablation for the periodic nanostructure formation.

Keywords: Periodic nanostructure; femtosecond laser pulses; near-field; surface plasmon polaritons; silicon surface

1. Introduction

In the last decade, a number of experimental studies have shown that intense femtosecond (fs) laser pulses produce periodic nanostructures on the surface of solids such as dielectrics [1–3], semiconductors [4–6] and metals [7,8], and also inside transparent materials [9,10], where the structure size observed is typically 1/10 – 1/5 of the laser wavelength λ used. Since the nanostructure formation observed for various kinds of solid materials suggests a new field of nanoscale, ultrafast light-matter interaction physics and its potential routes to laser nano-processing beyond the diffraction limit, much attention has been focused on the physical mechanism responsible for nanostructuring induced with fs laser pulses.

Formation of laser-induced surface structures with periodicities close to ~ λ has long been known as a universal phenomenon, so-called *ripples*, which is usually explained by the interference between

* Corresponding author. Tel.: +81-774-38-3470 ; fax: + 81-774-38-3472 .
E-mail address: miyazaki@iae.kyoto-u.ac.jp .

 doi:10.1016/j.phpro.2012.10.088

electromagnetic surface wave or surface plasmon and the incident light [11-13]. Since the traditional ripple formation mechanism can never account for the origin of nanoscale periodicity much smaller than λ, various mechanisms have been proposed so far. Those are concerned with self-organization of surface instability [2,14,15], second-harmonic generation [4,16], linear and/or nonlinear refractive index change [5,6,17], nanoplasma formation [10], and so on. The diverse discussion on the mechanism is due most likely to the fact that the nanostructuring strongly depends on fs-laser parameters, target materials, surface conditions, and ambient materials in contact with the target. The fundamental physics of periodic nanostructure formation is still being debated to make clear the exact mechanism.

To understand the detailed mechanism we have noted the experimental conditions that were used extensively for the formation of nanostructures, i.e., superimposed *multiple shots* of fs laser pulses at *lower fluence* than the single-pulse ablation threshold. Based on the experimental results obtained for diamond-like carbon (DLC) films [1,18-20], we have shown that low-fluence fs laser pulses induce *near-field* around high curvatures of small surface corrugation to initiate nanoscale ablation [19], and the origin of nano-periodicity can be attributed to the excitation of *surface plasmon polaritons* (SPPs) in the surface layer [20]. The model calculation reproduces well the observed nano-periodicity. In addition, the results suggest the non-thermal periodic energy deposition for nanostructuring [18,20].

The purpose of this study is to demonstrate that the excitation of SPPs is also the dominant mechanism for nanostructuring of silicon (Si) irradiated with fs laser pulses under the conditions of interest. For Si, several groups have reported so far the fs-laser-induced formation of periodic surface nanostructures [5,6,15,16,21-23]. The observed periodic structures much smaller than λ depended on the ambient materials, as Si targets were irradiated in water [5,6], oil [21,23], vacuum [15], and air [16,22], as well as on the laser parameters. In the previous studies, the nanostructuring of Si has been ascribed to various mechanisms mentioned above, suggesting need of further investigation to understand the exact process. We made the experimental study for crystalline Si (c-Si) immersed in water, because the low-repetition-rate fs laser used never produced the fine nanostructure in air. The results obtained show that the nanostructuring of Si can also be illustrated well with the excitation of SPPs in the surface layer. The pump-probe measurements of surface reflectivity strongly support this mechanism.

2. Experimental

Polished *p*-type c-Si (100) substrate of 380 μm in thickness was set in a small cell filled with distilled water, since the nanostructuring was observed only for the target in ambient liquids. The Si surface was irradiated through the 2-mm thick water layer and a thin quartz window of the cell, with linearly polarized, 800-nm, 100-fs laser pulses from a Ti:sapphire laser system operated at a repetition rate of 10 Hz. For the formation of periodic nanostructures, the laser beam having a well-defined Gaussian spatial profile was focused at normal incidence with a 1000-mm focal-length lens to the focal spot size $w_0 \sim 200$ μm in $1/e^2$ radius. The peak fluence $F = 2E_{\mathrm{pulse}}/\pi w_0^2$ on the target was estimated with the measured laser pulse energy E_{pulse} and w_0. In this experiment, F =100 – 200 mJ/cm^2, corresponding to E_{pulse} = 64 – 128 μJ. The fluence was smaller than the ablation threshold F_{th} and the melting or modification threshold F_{m} of c-Si for a single fs laser pulse at $\lambda \sim 800$ nm in air [5,24]. At the low fluence, more than a hundred superimposed shots of fs laser pulses were necessary for the onset of ablation.

The morphological change was observed with a scanning electron microscope (SEM). The SEM image was analyzed with the two-dimensional Fourier transform to see the distribution of periodicity.

3. Results and discussion

3.1. Formation of periodic nanostructures

Fig. 1 shows a pair of the SEM image and its frequency spectrum observed with the different superimposed shot number of fs laser pulses N at F = 120 mJ/cm^2. The image represents the line-like patterns extended to the direction perpendicular to the laser polarization vector, and the spectrum provides the distribution of the pattern period d measured along the laser polarization direction. The periodicity along the polarization is a spontaneous nature resulting from the enhanced near-field due to the excitation of SPPs, as discussed below.

In Fig. 1, the periodic structure starts to be formed in the central part of the focal spot at N = 400, where the spectrum represents a broad peak at d ~ 400 nm. With increasing N to 500, high frequency components grow up to form double peaks in the spectrum. With a further increase in N to 800 – 2000, the fine nanostructure with d ~ 150 nm rapidly develops to cover the whole area, as seen by the isolated sharp peak in the spectrum, while the coarse structure with d ~ 400 nm is greatly suppressed. This morphological change suggests that the fine nanostructure is efficiently produced *in succession to* the coarse structure, as if the coarse structure would be the source of the fine structure. It is noted that the periods of d ~ 150 nm and d ~ 400 nm are almost constant with an increase in N.

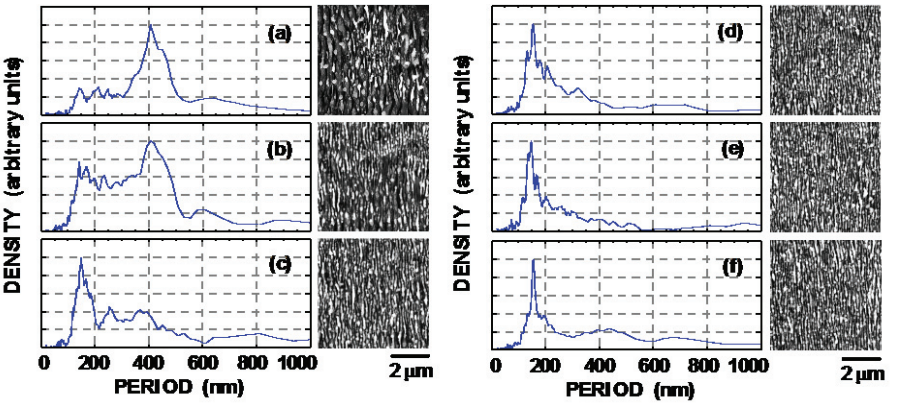

Fig. 1. SEM image of ablated Si surface and the distribution of structural period, observed with (a) N = 400, (b) N = 500, (c) N = 800, (d) N = 1200, (e) N = 1500, and (f) N = 2000 at F = 120 mJ/cm^2. The laser polarization direction is horizontal

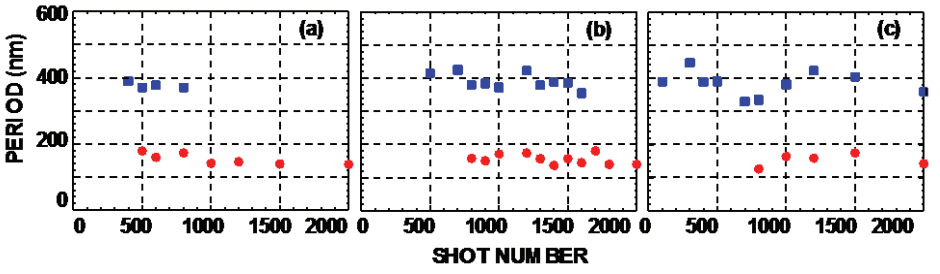

Fig. 2. Structural periods observed as a function of N at (a) F = 120 mJ/cm^2, (b) F = 130 mJ/cm^2 (b), and (c) F = 140 mJ/cm^2

For the c-Si in water, the fine nanostructure formation at $d \sim 150$ nm was observed only in a limited low-fluence range of $F = 120 - 140$ mJ/cm^2. The Si surface was never ablated at $F < 120$ mJ/cm^2, and only the coarse structure was formed at $F > 140$ mJ/cm^2. Fig. 2 plots the isolated peak position of d in the spectrum observed as a function of N at three different values of F. In the limited region of F, the periodic structure is mostly formed with two sizes of $d \sim 150$ nm and $d \sim 400$ nm. Note that the fine nanostructure formation is always preceded by the coarse structure as N increases, while an increase in F increases the additional number of pulses ΔN required for the fine nanostructure formation.

3.2. Nanostructuring process

The results shown in Figs. 1 and 2 demonstrate that multiple shots of fs laser pulses induce structural change to decrease the ablation threshold [5,18,24], while F is less than F_{th} for a single pulse. For c-Si, such multiple shots of low-fluence fs laser pulses are well known to produce an amorphous Si (a-Si) layer of a few tens of nanometers in thickness [24,25]. Since the absorption coefficient of a-Si is by an order of magnitude larger than that of c-Si [24], the laser energy density absorbed in the a-Si layer increases with an increase in N, resulting in the onset of random nanoscale ablation. In fact we observed such random ablation traces on Si, prior to the formation of periodic structure, as for DLC [20].

Thus, the Si target to be nanostructured can be modeled by a surface consisting of the a-Si and c-Si layers, as shown in Fig. 3(a), where the media a and c denote water and c-Si substrate with the relative dielectric constants ε_a and ε_c, respectively, and the medium b represents the a-Si layer formed on c-Si. The incident fs laser pulse predominantly produces a high density of free electrons N_e in the a-Si layer and induces an ultrafast change in the relative dielectric constant ε_b of the a-Si layer. On the surface corrugated with the initial random ablation, SPPs can transiently be excited via the coherent coupling of the incident laser pulse with the surface, where the a-Si layer including N_e works as a thin metal layer between water and the c-Si substrate for the excitation of SPPs [26].

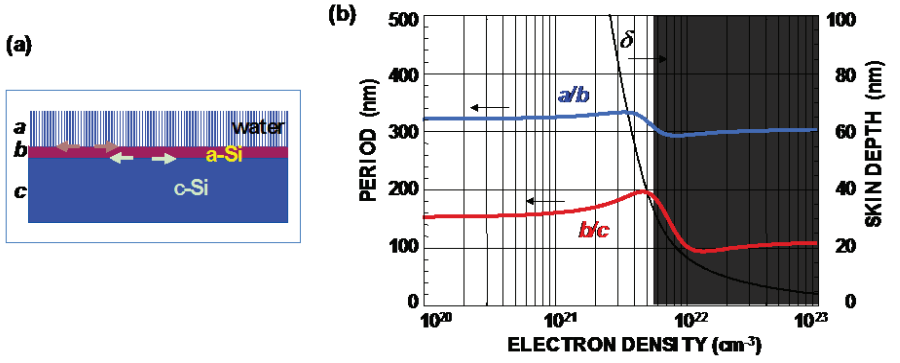

Fig. 3. (a) Model surface consisting of the a-Si layer and c-Si substrate; (b) structural periods at the water/a-Si interface (blue line) and at the a-Si/c-Si interface (red line), and the skin depth (black line) in the a-Si layer, calculated as a function of N_e. The shaded area denotes the region for possible excitation of SPPs

The excitation of SPPs is possible at two interfaces A (water/a-Si) and B (a-Si/c-Si) when the familiar dispersion relation

$$k_{spp} = k_0[\varepsilon_{a,c}\varepsilon_b'/(\varepsilon_{a,c} + \varepsilon_b')]^{1/2} \quad (1)$$

is satisfied [26], where k_{spp} is the plasmon wave number, k_0 is the wave number of the incident light in vacuum, $\varepsilon_{a,c}$ is ε_a or ε_c, and ε_b' is the relative dielectric constant of the layer b, including the effect of N_e. Using the Drude model, ε_b' in the laser field is written as $\varepsilon_b' = \varepsilon_b - [\omega_p^2/(\omega^2 + i\omega/\tau)]$, where ω is the incident light frequency in vacuum, τ is the Drude damping time of free electrons, and $\omega_p = [e^2N_e/(\varepsilon_0 m^* m)]^{1/2}$ is the plasma frequency with the dielectric constant of vacuum ε_0, the electron charge e and mass m, and the optical effective mass of carriers m^*.

When the SPPs are excited with fs laser pulses at normal incidence, localized near-field should be produced along the laser polarization direction at a period of the half SPP wavelength, $\lambda_{spp}/2 = (1/2)2\pi/(\mathrm{Re}\,[k_{spp}])$, due to the spatial standing wave. Using the published data of dielectric constants [27] and assuming $m^* = 0.2$ and $\tau = 1$ fs [28], we calculated λ_{spp}. Fig. 3(b) shows the results of $\Lambda = \lambda_{spp}/2$ as a function of N_e for the interfaces A and B, together with the skin depth δ in the layer b. The condition of $\varepsilon_b' < 0$ has to be satisfied for the excitation of SPPs [26], which corresponds to the shaded region of N_e * 5.5 * 10^{21} cm^{-3} in Fig. 3(b). As described below, we have confirmed that the ablation for nanostructuring certainly takes place at N_e in this region. The calculated periods are $\Lambda \sim 300$ nm for the interface A and $\Lambda = 100 – 200$ nm for the interface B, being in good agreement with the observed coarse and fine periods of $d \sim 400$ nm and ~ 150 nm, respectively. In more detail, however, the calculated value of d at the interface A is smaller than the observed one. This is most likely due to the simplified modeling of the target, where we have disregarded the thin SiO_2 layer that is usually present on the surface of c-Si substrate [23,24].

As seen in Fig. 3(b), the calculated skin depth δ in the a-Si layer rapidly decreases down to $\delta \sim 35$ nm, as N_e increases up to $N_e \sim 5.5$ * 10^{21} cm^{-3}. This critical value of δ is consistent with the a-Si layer thickness (38 – 42 nm) observed for the c-Si surface irradiated with fs laser pulses [24,25]. Referring to the calculated results, we can explain the characteristic behavior of ΔN in the fine and coarse structure formations in Fig. 2. A higher fluence of fs laser pulses would create a thicker a-Si layer before ablation. When the a-Si layer thickness exceeds the critical value of δ, the excitation of SPPs at the interface B would hardly be induced. For the fine nanostructure formation, the a-Si layer thickness must be reduced through the ablation with the additional shots of fs pulses ΔN, while the coarse structure is formed at the interface A. Thus a higher value of F leads to an increase in ΔN for the fine nanostructure formation, as seen in Fig. 2. In addition, the higher fluence increases the energy deposited into the surface layer and resulting thermal effects to restrict the fine structure formation.

3.3. The role of superimposed multiple shots

The SEM images observed include little information about the surface condition before ablation. To see the role of multiple shots of fs laser pulses in nanostructuring, we measured the temporal change of the reflectivity $R(\Delta t)$ of Si surface in water, using a pump-probe technique with the time delay Δt between the pump and probe pulses. The optical configuration is briefly shown in Fig. 4(a). The p-polarized pump beam, obliquely incident at the angle of 12°, was focused to the spot size $w_0 = 115$ μm, while the orthogonally polarized probe pulse was incident at normal to cover the whole pumped area. Every shot of the reflected probe pulse was recorded with a CCD camera, and $R(\Delta t)$ was measured for the central pump beam area of 40-μm in diameter.

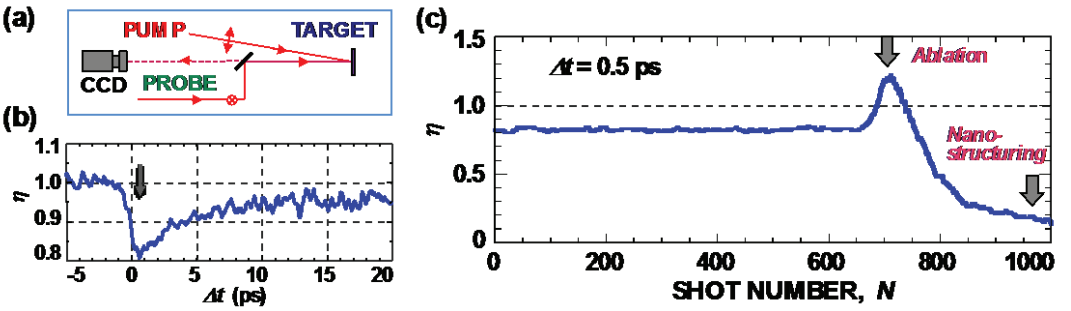

Fig. 4. (a) Configuration for the pump-probe measurement of the reflectivity ; (b) the temporal change of $\eta = P/P_0$ observed with a single fs laser pulse; (c) η measured as a function of the shot number N at $\Delta t = 0.5$ ps. $F = 120$ mJ/cm^2 in (b) and (c)

Fig. 4(b) shows the temporal change in $\eta = R/R_0$ for a single pump pulse at $F = 120$ mJ/cm^2, where $R_0 = 22.1$ % is the original reflectivity of the non-irradiated c-Si surface in water. In this single-pulse experiment, the target was translated shot by shot so that each pump pulse hits a fresh surface area. As seen in Fig. 4(b), a single pump pulse induces the rapid decrease of η to ~ 0.8 at $\Delta t \sim 0.5$ ps, representing the generation of high-density free electrons on the surface. After the pump-pulse interaction, η slowly decays due primarily to the energy transfer from free electrons to the lattice [29]. Using the Drude expression, we can estimate as $N_e \sim 1.0 * 10^{21}$ cm^{-3} for the minimum of η at $\Delta t \sim 0.5$ ps.

Keeping the time delay at $\Delta t = 0.5$ ps, η was measured as a function of the superimposed shot number N of pump pulses at the same fluence. The result is shown in Fig. 4(c). With increasing N, the initial value of η ~ 0.8 is almost constant up to $N \sim 600$, while no morphological change on the target surface was observed. With a further increase in N, η rapidly grows up to η~ 1.2 at $N \sim 700$. This enhancement of η certainly indicates the onset of ablation, corresponding to the result for $N = 400$ in Fig. 1, whereas the experimental conditions are slightly different. After the ablation takes place on the surface, η is observed to monotonously decrease with an increase in N, most likely due to the increase in absorption and scattering on the surface. Finally, the low-fluence fs laser pulses form the fine periodic nanostructure with $d \sim 150$ nm at $N \sim 1000$. Thus the results shown in Fig. 4(c) demonstrate that the bonding structural change is certainly accumulated in the region of $N < \sim 700$, and then a high electron density to initiate the ablation brings about the abrupt enhancement of η at $N \sim 700$. We estimated $N_e = (0.6 – 1.0)$ [illegible] cm^{-3} for the peak value η ~ 1.2, assuming a thin a-Si layer. This value is consistent with N_e for the possible excitation of SPPs in Fig. 3(b).

3.4. Thermal effects

The same experiments as in water were made for c-Si in air. The results have shown that only a ripple-like structure with $d \sim 600$ nm was produced at the higher ablation threshold by about 30 % than in water. This suggests that the formation of fine nanostructures is limited in air by the thermal effect [29,30], since the fine nanostructure is formed in water at the lower fluence of $F = 120 – 140$ mJ/cm^2. In air, the excess energy must be deposited into the a-Si layer and would destroy the fine energy distribution at the interface B. We have confirmed such thermal effects in the pump-probe measurement of η. The results will be reported in detail elsewhere.

Recently, the fine nanostructure formation on Si was observed even in air with high-repetition rate (80 MHz) fs laser pulses [16,22]. In the experiment, the thermal effect to destroy the fine periodicity might effectively be suppressed by scanning the tightly focused fs laser beam.

3.5. Mechanism of nanostructuring - summary

The nanostructuring of c-Si surface may be summarized as illustrated in Fig. 5: (a) Each shot of low-fluence fs laser pulses induces the bonding structural change from c-Si to a-Si. As the a-Si density increases in the surface, the laser energy density absorbed in the a-Si layer increases to bring about nanoscale random ablation of the surface; (b) The random ablation creates nanoscale surface corrugation to induce strong *near-field* around the high curvatures along the laser polarization direction. The near-field increases ablation traces to produce high-frequency surface components along the field direction; (c) The surface corrugation can coherently couple the incident field with the collective oscillation of free electrons in the surface layer to excite SPPs. The standing wave of SPPs would easily be formed along the laser polarization in the focal area; (d) At the low fluence, the nanoscale periodic energy deposition should be maintained in the surface layer for 10 – 100 ps until the onset of ablation, so that the periodic surface nanostructure is formed with the periodicity of ~ $\lambda_{SPP}/2$. Non-thermal developments of these processes are crucial to the nanostructuring.

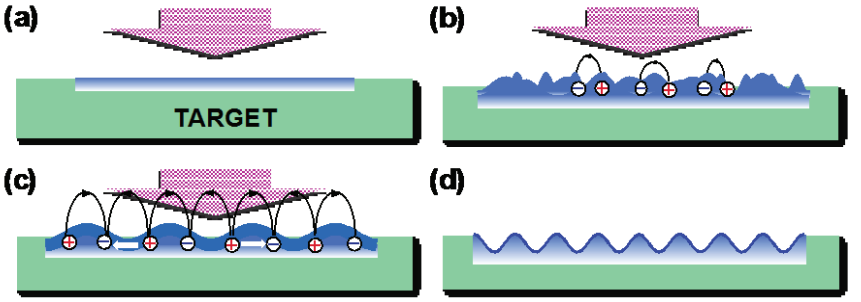

Fig. 5. Nanostructuring process on Si surface irradiated with multiple shots of low-fluence fs laser pulses in water

The mechanism of nanostructuring based on the excitation of SPPs should be valid for different kinds of solid materials irradiated with fs laser pulses under the conditions concerned.

Acknowledgements

The authors thank K. Zhang, T. Yoshifuji, and J. Fujita for their cooperation in the preliminary stage of this work. This work is partially supported by the Grant-in-Aid for Scientific Research 23360034, 22110506, and 24686011.

References

[1] Yasumaru, N.; Miyazaki, K.; Kiuchi, J.: Femtosecond-laser-induced nanostructure formed on hard thin films of TiN and DLC. *Appl. Phys. A* 2003; **76**: pp. 983–5.

[2] Reif, J.; Costache, F.; Henyk, M.; Pandelov, S.V.: Ripples revisited: non-classical morphology at the bottom of femtosecond laser ablation craters in transparent dielectrics. *Appl. Surf. Sci.* 2002; **197**–**198**: pp. 891–5.

[3] Dong Y.; Molian, P.: Coulomb explosion-induced formation of highly oriented nanoparticles on thin films of 3C–SiC by the femtosecond pulsed laser. *Appl. Phys. Lett.* 2004; **84**: pp. 10–2.

[4] Borowiec A.; Haugen, H.K.: Subwavelength ripple formation on the surfaces of compound semiconductors irradiated with femtosecond laser pulses. *Appl. Phys. Lett.* 2003; **82**: pp. 4462–4.

[5] Daminelli, G.; Krüger, J.; Kautek, W.: Femtosecond laser interaction with silicon under water confinement. *Thin Solid Films* 2004; **467**: pp. 334–41.

[6] Wang, C.; Huo, H.; Johnson, M.; Shen, M.; Mazur, E.: The thresholds of surface nano-/micro-morphology modifications with femtosecond laser pulse irradiations. *Nanotechnology* 2010; **21**: pp. 075304/1–5.

[7] Zhao, Q.Z.; Malzer, S.; Wang, L.J.: Formation of subwavelength periodic structures on tungsten induced by ultrashort laser pulses. *Opt. Lett.* 2004; **32**: pp.1932–4.

[8] Golosov, E.V.; Emel'yanov, V.I.; Ionin, A.A.; Kolobov, Yu.R.; Kudryashov, S.I.; Ligachev, A.E.; Novoselov, Yu.N.; Seleznev, L.V.; Sinitsyn, D.V.: Femtosecond Laser Writing of Subwave One Dimensional Quasiperiodic Nanostructures on a Titanium Surface. *JETP Lett.* 2009; **90**: pp. 107–10.

[9] Shimotsuma, Y.; Kazansky, P.G.; Qiu, J.; Hirao, K.: Self-Organized Nanogratings in Glass Irradiated by Ultrashort Light Pulses. *Phys. Rev. Lett*. 2003; **91**: pp. 247405/1–4.

[10] Bhardwaj, V.R.; Simova, E.; Rajeev, P.P.; Hnatovsky, C.; Taylor, R.S.; Rayner, D.M.; Corkum, P.B.: Optically Produced Arrays of Planar Nanostructures inside Fused Silica. *Phys. Rev. Lett.* 2006; **96**: pp. 057404/1–4.

[11] Siegman A.E.; Faucher, P.M.: Stimulated Wood's Anomalies on Laser-Illuminated Surfaces. *IEEE J. Quantum Electron.* 1986; **QE-22**: pp. 1384–1403, and references therein.

[12] Bonse, J.; Rosenfeld, A.; J. Krüger: On the role of surface plasmon polaritons in the formation of laser-induced periodic surface structures upon irradiation of silicon by femtosecond laser pulses. *J. Appl. Phys.* 2009; **106**: pp. 104910/1–5.

[13] Huang, M.; Zhao, F.; Cheng, Y.; Xu, N.; Xu, Z.: Origin of Laser-Induced Near-Subwavelength Ripples: Interference between Surface Plasmons and Incident Laser. *ACS Nano* 2009; **3**: pp. 4062–70.

[14] Varlamova, O; Costache, F.; Reif, J.; Bestehorn, M.: Self-organized pattern formation upon femtosecond laser ablation by circularly polarized light. *Appl. Surf. Sci.* 2006; **252**: pp. 4702–6.

[15] Costache, F.; Kouteva-Arguirova, S.; Reif, J.: Sub-damage-threshold femtosecond laser ablation from crystalline Si: surface nanostructures and phase transformation. *Appl. Phys. A* 2004; **79**: pp. 1429–32.

[16] Harzic, R.Le; Dörr, D.; Sauer, D.; Stracke, F.; Zimmermann, H.: Generation of high spatial frequency ripples on silicon under ultrashort laser pulses irradiation. *Appl. Phys. Lett.* 2011; **98**: pp. 211905/1–3.

[17] Wu, Q.; Ma, Y.; Fang, R.; Liao, Y.; Yu, Q.; Chen, X.; Wang, K.: Femtosecond laser-induced periodic surface structure on diamond film. *Appl. Phys. Lett.* 2003; **82**: pp. 1703–5.

[18] Miyazaki, K.; Maekawa, N.; Kobayashi, W.; Yasumaru, N.; Kiuchi, J.: Reflectivity in femtosecond-laser-induced structural changes of diamond-like carbon film. *Appl. Phys. A* 2005; **80**: pp. 17–21.

[19] Miyaji, G.; Miyazaki, K.: Nanoscale ablation on patterned diamondlike carbon film with femtosecond laser pulses. *Appl. Phys. Lett.* 2007; **91**: pp. 123102/1–3.

[20] Miyaji, G.; Miyazaki, K.: Origin of periodicity in nanostructuring on thin film surfaces ablated with femtosecond laser pulses. *Opt. Express* 2008; **16**: pp. 16265–71.

[21] Harzic, R.Le; Schuck, H.; Sauer, D.; Anhut, T.; Riemann, I.; König, K.: Sub-100 nm nanostructuring of silicon by ultrashort laser pulses. *Opt. Express* 2005; **13**: pp. 6651–6.

[22] Harzic, R.Le; Dörr, D.; Sauer, D.; Neumeier, M.; Epple, M.; Zimmermann, H.; Stracke, F.: Large-area, uniform, high-spatial-frequency ripples generated on silicon using a nanojoule-femtosecond laser at high repetition rate. *Opt. Lett.* 2011; **36**: pp. 229–31.

[23] Straub, M.; Afshar, M.; Feili, D.; Seidel, H.; König, K.: Periodic nanostructures on Si(100) surfaces generated by high-repetition rate sub-15 fs pulses near-infrared laser light. *Opt. Lett.* 2012; **34**: pp. 190-2.

[24] Bonse, J.; Brzezinka, K.-W. ; Meixner, A.J.: Modifying single-crystalline silicon by femtosecond laser pulses: an analysis by micro Raman spectroscopy, scanning laser microscopy and atomic force microscopy. *Appl. Surf. Sci.* 2004; **221**: pp. 215–30.

[25] Izawa, Y.; Izawa, Y.; Setsuhara, Y.; Hashida, M.; Fujita, M.; Sasaki, R.; Nagai, H.; Yoshida, M.: Ultrathin amorphous Si layer formation by femtosecond laser pulse irradiation. *Appl. Phys. Lett.* 2007; **90**: 044107/1–3.

[26] Raether H.: *Surface Plasmons on Smooth and Rough Surfaces and on Gratings*. Berlin: Springer; 1988.

[27] Palik, E.D.: *Handbook of Optical Constants of Solids*. London: Academic; 1997.

[28] Sokolowski-Tinten K.; von der Linde, D.: Generation of dense electron-hole plasmas in silicon. *Phys. Rev. B* 2000; **61**: 2643–50.

[29] Shank, C.V.; Yen, R.; Hirlimann, C.: Time-Resolved Reflectivity Measurements of Femtosecond-Optical-Pulse-Induced Phase Transitions in Silicon. *Phys. Rev. Lett.* 1983; **50**: pp. 454–7.

[30] Sokolowski-Tinten, K.; Bialkowski, J.; Cavalleri, A.; von der Linde, D.; Oparin, A.; Meyer-ter-Vehn, J.; Anisimov, S.I.: Transient States of Matter during Short Pulse Laser Ablation. *Phys. Rev. Lett.* 1998; **81**: pp. 224–7.